JOURNAL OF MATERIALS SCIENCE 25 (1990) 1416–1422

Structural characteristics and optical properties of vestan (polyester) fibres

I. M. FOUDA, M. M. EL-TONSY, A. H. ORABY
Physics Department, Faculty of Science, Mansoura University, Mansoura, Egypt

Refractive indices and birefringence for skin and core changes with strain, produced by different stresses in undrawn vestan fibres, were measured interferometrically. Applications were carried out using multiple-beam Fizeau fringes in transmission to determine the Cauchy's constants and dispersive coefficient for the fibre layers. The resulting data were used to calculate the polarizability per unit volume for each layer. The scanning electron microscope (SEM), optical microscope and He–Ne laser beam were applied to estimate the geometrical parameters of the fibre cross-section. A comparative study between the three methods used for measuring the fibre diameter was made. The effect of temperature on the refractive index and birefringence for each fibre layer has been also investigated. The relationship between temperature and birefringence of the fibres was studied and the thermal coefficient of the refractive index was determined. An empirical formula is suggested to relate temperature and birefringence. Illustrations are given using microinterferograms.

1. Introduction

Interference microscopy has been applied to the study of surface topography and optical parameters of fibres. When certain textile fibres are examined microscopically, their size, cross-sectional shape and characteristic markings permit the observer to identify them. However, the successful identification of fibres, or the proof that two fibres are similar, is more difficult when fibres are regular in outline and free from significant markings. Various optical properties such as refractive index and birefringence are recognized in fibres as the main source of accurate information on the structural properties of synthetic fibres related to their method of production. The refractive index is a measure of velocity of light in the medium and is related to the polarizability of the chains. Birefringence is used routinely in many industrial film and fibre plants as a measure of the average orientation of the sample. Thus the final measurement of birefringence is a function of contribution of polarizabilities of all molecular units in the sample [1]. Consequently the birefringence measurement is a rapid and powerful tool for studying the morphological characteristics of synthetic fibres. Birefringence gives a measure of orientation which is an average of that of the amorphous and crystalline regions [2].

In recent years, interferometric methods have been used to determine the indices of refraction and birefringence of both natural and man-made fibres [3–11].

2. Experimental procedures and discussion

In this work, three different techniques were used to estimate the geometrical parameters of vestan (polyester) fibres. The scanning electron microscope, optical microscope and the diffraction of a He–Ne laser beam were used to measure the dimensional parameters and transverse sectional shape [12, 13].

The interferometric technique was utilized to study the optical properties of these fibres. The technique has been described in detail previously [3, 5]. The change of the refractive indices and birefringence of the fibre layers to the applied mechanical drawing were studied using a micro-strain device provided with a wedge interferometer, as discussed elsewhere [14], to produce multiple-beam Fizeau fringes in transmission.

In this study, the techniques and relations used are listed below.

2.1. Transverse-sectional shape and diameter measurement

2.1.1. Scanning electron microscope (SEM)

A bundle of vestan (polyester) fibres was examined. The cross-sectional shape is shown in Fig. 1. The mean fibre diameter was found to be $39.8 \pm 1.40\,\mu m$.

2.1.2. Optical cross-section method

Figure 2 shows the optically obtained cross-sectional shape of the vestan fibres. The mean diameter was found to be $39.7 \pm 1.90\,\mu m$.

2.1.3. Diffraction of He–Ne laser beam

In this method the following formula [12, 13] is used:

$$d = \pm \lambda l / x \qquad (1)$$

where d is the fibre thickness; $\lambda = 632.8\,nm$ (the wavelength of the He–Ne laser used); x the distance from the centre of the pattern to the first minimum; and l the distance between the fibre and the screen on which the diffraction pattern is produced. Twenty-five samples were examined. Figure 3 shows the graphical plot of cross-sectional shape for six different samples.

0022–2461/90 $03.00 + .12

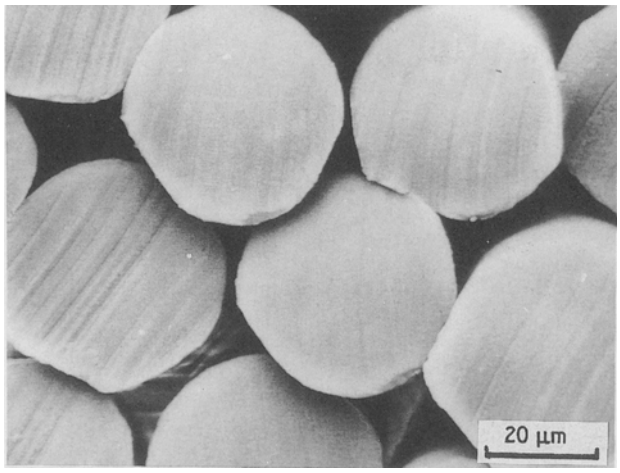

Figure 1 Cross-section of vestan (polyester) fibres as seen in the SEM.

The mean fibre diameter was found to be $39.4 \pm 1.30\,\mu m$.

2.2. Interferometric measurement of the optical parameters

Multiple-beam Fizeau fringes in transmission were used for the determination of the basic optical parameters of vestan (polyester) fibres.

2.2.1. Determination of refractive indices and birefringence for the fibre layers

For the determination of the refractive index of each layer, n_k, of a cylindrical fibre having m layers of circular cross-sections, El-Nicklawy and Fouda [5] derived an expression for the size of the fringe shift δz at any point x along the diameter of a multi-skin fibre. In a case having only skin–core fibre, their expression leads to the following formula:

$$(\lambda/4h)\,\delta z = (n_s^{\parallel} - n_L)(r_s^2 - x^2)^{1/2} + (n_c^{\parallel} - n_s^{\parallel})(r_c^2 - x^2)^{1/2} \quad (2)$$

where $n_s^{\parallel}$ and $n_c^{\parallel}$ are refractive indices of skin and core, respectively, for plane polarized light vibrating parallel to the fibre axis; n_L is the refractive index of the immersion liquid; r_s and r_c are the radii of skin and core layers, respectively; h is the liquid interfringe spacing; and λ is the wavelength of the monochromatic light used. An analogous formula for Equation 2 is used for plane-polarized light vibrating perpendicular to the fibre axis, to the determination of both $n_s^{\perp}$ and $n_c^{\perp}$.

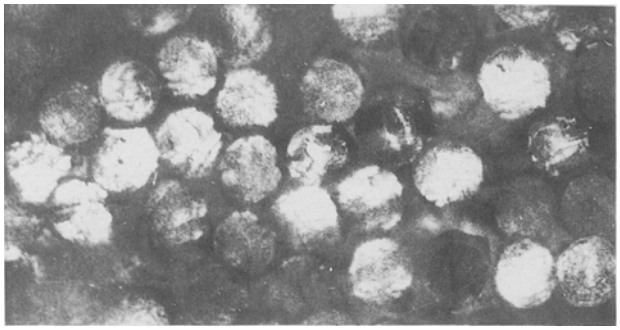

Figure 2 Cross-section of vestan fibres as seen under the optical microscope.

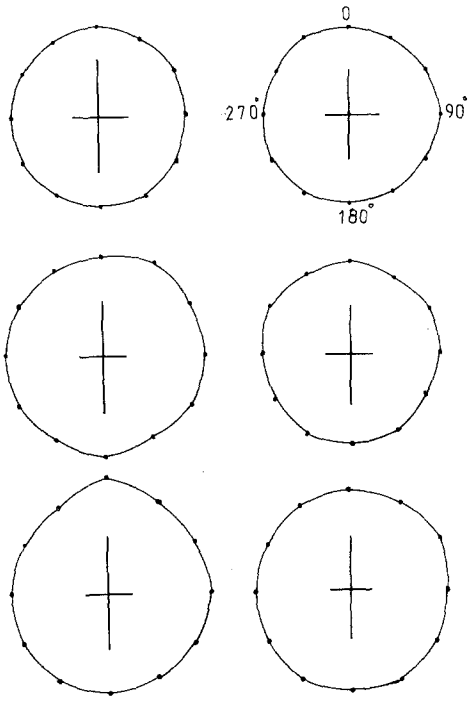

Figure 3 Graphical cross-section shape of vestan fibres as measured by laser beam forward diffraction.

2.2.2. The mean refractive index n_a

The mean refractive index n_a of vestan fibres, having a core of thickness t_c and refractive index n_c, surrounded by a skin layer of thickness t_s and refractive index n_s, is calculated using the formula [3]:

$$n_a = n_c \frac{t_c}{t_f} + n_s \frac{t_s}{t_f} \quad (3)$$

where t_f is the whole fibre thickness.

2.2.3. The dispersion of vestan fibres

The dispersion properties of the fibres under test are studied using the well-known Cauchy's formula:

$$n(\lambda) = A + B/\lambda^2 \quad (4)$$

where A and B are Cauchy's constants.

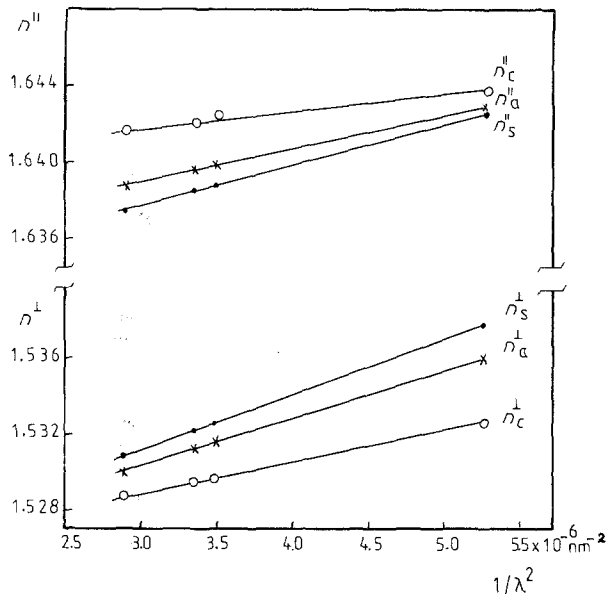

Figure 4 Variation of $n_s^{\parallel}$, $n_s^{\perp}$, $n_c^{\parallel}$, $n_c^{\perp}$, $n_a^{\parallel}$ and $n_a^{\perp}$ with $1/\lambda^2$.

TABLE I Values of Cauchy's constants for vestan fibre layers in the two principal directions of vibration of light

Layer	$A^{\parallel}$	$A^{\perp}$	$B^{\parallel}$ (nm^2)	$B^{\perp}$ (nm^2)
Skin	1.6367	1.5297	2100	2900
Core	1.6412	1.5280	1000	1700
Mean	1.6382	1.5311	1700	2500

The refractive indices $n(\lambda)$ of vestan fibres are measured interferometrically. Figure 4 shows the variations of $n_s^{\parallel}$, $n_s^{\perp}$, $n_c^{\parallel}$, $n_c^{\perp}$, $n_a^{\parallel}$ and $n_a^{\perp}$ with $1/\lambda^2$ from which Cauchy's constants are determined. Table I gives values of Cauchy's constants for both layers of vestan fibres in the two principal directions of vibration of the light. Figure 5 shows the change of birefringence Δn_s, Δn_c and Δn_a with $1/\lambda^2$.

2.2.4. The dispersive coefficient of vestan fibres

The dispersive coefficient ($dn/d\lambda$) can be obtained by differentiating Equation 4, i.e.:

$$dn(\lambda)/d\lambda = -2B/\lambda^3 \quad (5)$$

Table II gives values of the dispersive coefficient for layers of the vestan fibres in the two directions of polarization for the used monochromatic light beams.

2.2.5. Refractive index – draw ratio dependence of vestan fibres

The micro-strain device as designed and used in [14] was used in this study. The refractive indices $n^{\parallel}$ and $n^{\perp}$ for the fibre layers and also their mean values are determined interferometrically at different draw ratios. Figures 6a–c are microinterferograms of multiple-beam Fizeau fringes in transmission for vestan fibres with draw ratios of 1.000, 1.072 and 1.120, respectively. Monochromatic light of wavelength 546.1 nm vibrating parallel to the fibre axis was used at 33.5° C. Figures 7a–c are microinterferograms of multiple-beam Fizeau fringes in transmission for vestan fibres with draw ratios of 1.021, 1.043 and 1.064, respectively. Monochromatic light of wavelength 546.1 nm vibrating perpendicular to the fibre axis was used at 33.5° C.

Figure 8 shows the behaviour of the refractive indices $n_s^{\parallel}$, $n_c^{\parallel}$ and $n_a^{\parallel}$ of vestan fibres through the allowed range of drawing before the cut-off of the fibre. Figure 9 illustrates the change of birefringence of the skin and core layers as well as their mean value for vestan fibres when increasing the draw ratio. Table III gives the experimental values of refractive indices of the skin and core of the vestan fibres and their birefringence at different draw ratios.

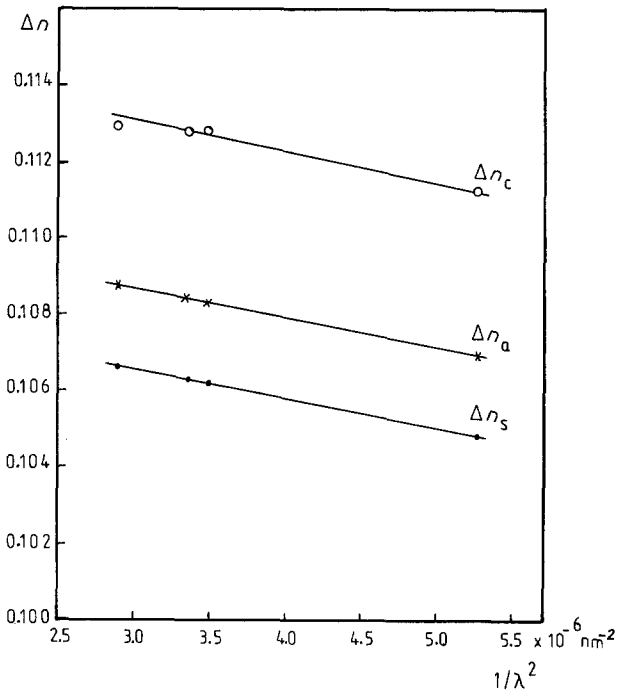

Figure 5 Variation of Δn_s, Δn_c and Δn_a with $1/\lambda^2$.

2.2.6. The polarizability per unit volume

The experimental values of the refractive indices were utilized to obtain the polarizability per unit volume, using Lorntz–Lorenz equation:

$$P^{\parallel} = 3(n_{\parallel}^2 - 1)/4\pi(n_{\parallel}^2 + 2) \quad (6)$$

and with an analogous formula for the perpendicular direction. Table IV shows the calculated values of polarizability per unit volume for the skin and core of vestan fibres, and their mean values for light vibrating parallel and perpendicular to the fibre axis.

2.2.7. Refractive index – temperature dependence of vestan fibres

The multiple-beam Fizeau fringes were used to study the thermal change of refractive index and birefringence for skin and core layers of vestan fibres. The produced fringe shift has been measured through the change of temperature within the range 42 to 18° C with tolerance of ± 0.5° C.

Figures 10a–e are microinterferograms showing the variation of fringe shift across the vestan fibre at temperatures of 41.5, 38, 28, 21.5 and 18° C, respectively. A monochromatic light, wavelength 546.1 nm vibrating parallel to the fibre axis was used.

Figure 11 gives the behaviour of the refractive indices $n_s^{\parallel}$, $n_c^{\parallel}$ and $n_a^{\parallel}$ of vestan fibre with different temperatures. It is clear that both $n_s^{\parallel}$ and $n_a^{\parallel}$ obey nearly inversely linear behaviour with temperature. The refractive

TABLE II Dispersive coefficients for vestan fibre layers at different wavelengths

λ (nm)	$-(dn/d\lambda)^{\parallel}$ (nm^{-3})			$-(dn/d\lambda)^{\perp}$ (nm^{-3})		
	Skin	Core	Mean	Skin	Core	Mean
589.3	2.05×10^{-5}	0.98×10^{-5}	1.66×10^{-5}	2.83×10^{-5}	1.66×10^{-5}	2.44×10^{-5}
546.1	2.58×10^{-5}	1.23×10^{-5}	2.09×10^{-5}	3.56×10^{-5}	2.09×10^{-5}	3.07×10^{-5}
535.1	2.74×10^{-5}	1.31×10^{-5}	2.22×10^{-5}	3.79×10^{-5}	2.22×10^{-5}	3.26×10^{-5}
436.0	5.07×10^{-5}	2.41×10^{-5}	4.10×10^{-5}	7.00×10^{-5}	4.10×10^{-5}	6.03×10^{-5}

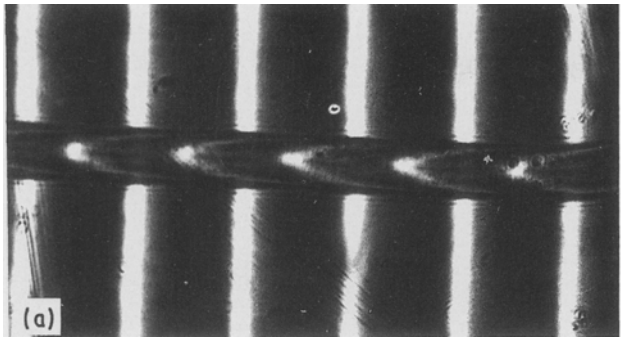

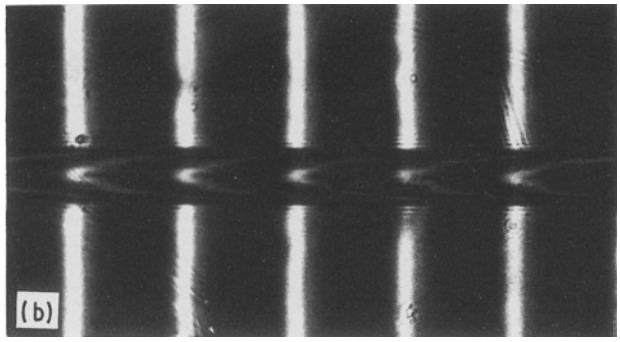

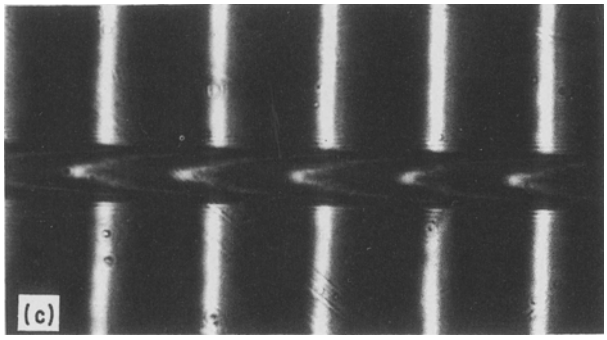

Figure 6 Microinterferograms of multiple-beam Fizeau fringes in transmission crossing vestan fibres, as different draw ratios for light vibrating parallel to the fibre axis.

index of the fibre core for light vibrating parallel to the fibre axis, $n_c^{\parallel}$, suffers a drop as the temperature exceeds 28° C, which means that the molecular orientation of the core medium quickly changes, becoming closer to the orientation of the skin medium.

Figure 12 shows the behaviour of refractive indices $n_s^{\perp}$, $n_c^{\perp}$ and $n_a^{\perp}$ of vestan fibres with different temperatures. It is clear that all refractive indices of vestan fibre for light vibrating perpendicular to the fibre axis are decreased nearly linearly as the temperature increases. Table V gives the experimental values of the mean thermal coefficient of the refractive index (dn/dT) of the vestan fibre layers within two temperature ranges. It is found that the birefringence of the core and skin media, and accordingly the mean birefringence, decrease as the temperature of the fibre exceeds room temperature (27° C). On the other hand, values of the birefringence Δn_c, Δn_s and Δn_a are nearly steady at temperatures lower than room temperature. So an empirical formula is suggested to give values of birefringence of vestan (polyester) fibres at temperatures higher than room temperature:

$$\Delta n(T) = \Delta n(r) \exp -(1 - T(r)/T)^{\beta} \qquad (7)$$

where $\Delta n(T)$ is the birefringence at temperature T; $\Delta n(r)$ is the steady birefringence at room temperature $T(r)$; and β is a constant characterizing the fibre layer. This formula is applicable for core, skin and also for the mean birefringence. The experimental results show that

for the fibre core, $\Delta n_c(r) = 0.1142$, $\beta_0 = 2.4$

for the fibre skin, $\Delta n_s(r) = 0.0985$, $\beta_s = 4.2$

for the mean index, $\Delta n_a(r) = 0.1034$, $\beta_a = 3.2$

Figure 13 illustrates the fair agreement between the theoretical values of $\Delta n(T)$ for core, skin and mean birefringence (full curves) of vestan fibres and the experimental values (separate points). Theoretical values are calculated using the empirical formula in Equation 7, noting that the tolerance in measuring the temperature is ± 0.5° C and that in measuring birefringence is ± 0.0006°. In general, the refractive indices and birefringence of vestan fibres are inversely proportional to temperature and are found to be in accordance with the suggested empirical formula. The

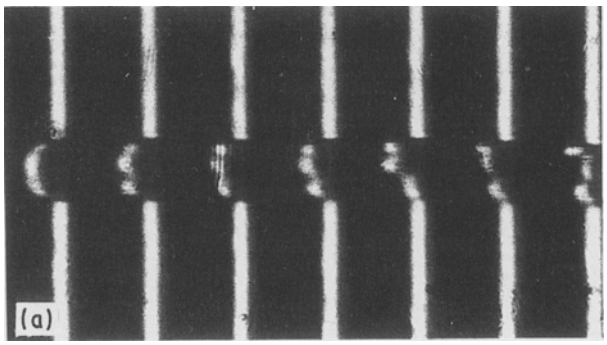

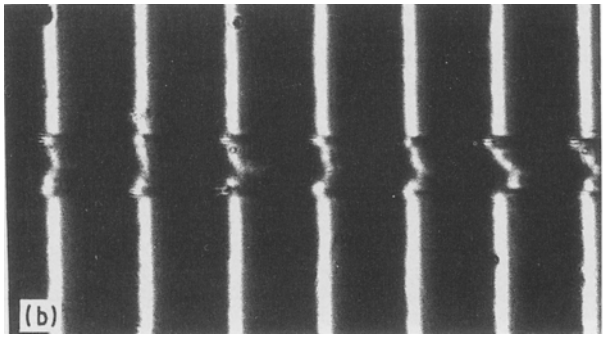

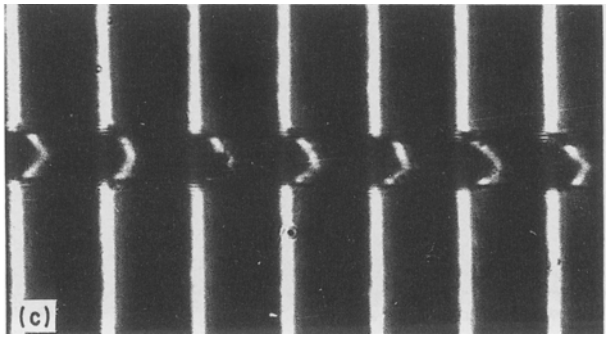

Figure 7 Microinterferograms of multiple-beam Fizeau fringes in transmission crossing vestan fibres, at different draw ratios for light vibrating perpendicular to the fibre axis.

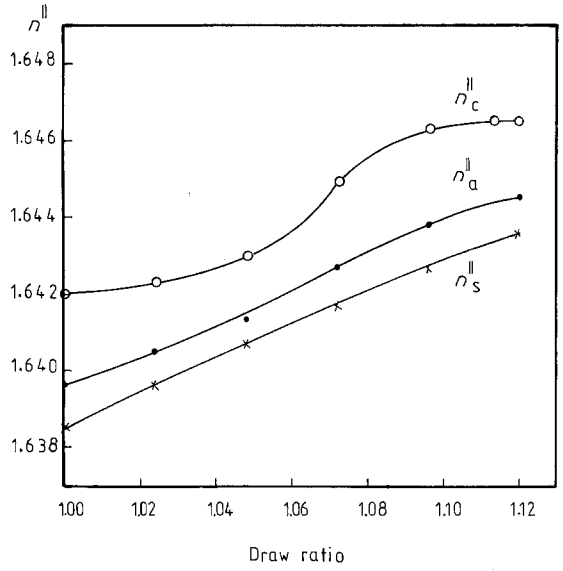

Figure 8 Changes of $n_s^{\parallel}$, $n_c^{\parallel}$ and $n_a^{\parallel}$ due to changes in the draw ratio R.

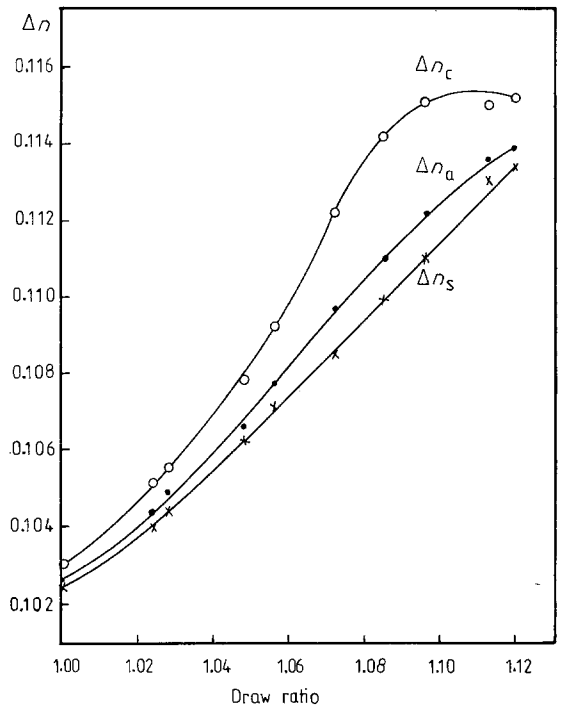

Figure 9 Changes of birefringence Δn_s, Δn_c and Δn_a due to increased draw ratio R.

results described here demonstrate the importance of the effect of temperature on the optical properties of vestan fibres. Hence the radiative properties of the medium used must be properly defined with respect to the fibre orientation, size distribution and optical properties [15].

This work demonstrates the applicability of Equations 2 and 3 for determining the basic parameters of vestan (polyester) fibres with a circular skin–core cross-sectional shape. It has been shown that the surface of a fibre (skin) is different from its core. This difference has been variously described as a greater degree of orientation or greater degree of crystallinity created in the fibre skin. While passing through the spinnerets, that part of the spinning solution which is in contact with the sides of the orifice will be subject to more frictional resistance than the solution in the centre of the orifice. The extra resistance encountered by the spinning solution in contact with the edge of the orifice lines up the long molecules and changes their orientation or crystallinity [16].

Recent applications of this mathematical expression in calculating the basic parameters of fibres provide accurate information about different orientations arranged in the fibre.

Three different techniques were used to estimate the cross-sectional shape and the fibre diameter. The forward-light diffraction technique is more practical owing to the time advantage. Moreover, the results obtained by this method are more accurate and sensitive than those obtained by the other two methods. Also, the diffraction technique has the advantage that it does not involve the cutting or pulling of fibres through the slits, which would cause deformations. The technique facilitates the estimation of fibre cross-sectional shape from a graphical plot of the fibre radius vector against the angle of rotation of the fibre around the axis. Diffraction is sensitive to any change in the cross-sectional shape within a limit error of 0.02%, while for the optical technique (metal-plate method) the cross-sectional shape error is 2%, and for the scanning electron microscopic technique, it is 0.1%.

3. Conclusion

From these measurements relating the change of optical properties to external strain and thermal effect in vestan fibres, the following conclusions may be drawn.

1. The microinterferograms are clear to identify differences in optical path variations due to undrawn and drawn fibres.

TABLE III Refractive indices $n_c^{\parallel}$, $n_c^{\perp}$, $n_s^{\parallel}$, $n_s^{\perp}$, $n_a^{\parallel}$, $n_a^{\perp}$ and birefringence Δn_c, Δn_s and Δn_a for a vestan fibre at different draw ratios

Draw ratio	$n_c^{\parallel}$	$n_c^{\perp}$	Δn_c	$n_s^{\parallel}$	$n_s^{\perp}$	Δn_s	$n_a^{\parallel}$	$n_a^{\perp}$	Δn_a
1.000	1.6420	1.5390	0.1030	1.6385	1.5361	0.1024	1.6396	1.5370	0.1026
1.024	1.6423	1.5372	0.1051	1.6396	1.5356	0.1040	1.6405	1.5361	0.1044
1.028	1.6424	1.5369	0.1055	1.6399	1.5355	0.1044	1.6408	1.5359	0.1049
1.048	1.6430	1.5352	0.1078	1.6407	1.5345	0.1062	1.6413	1.5347	0.1066
1.056	1.6433	1.5341	0.1092	1.6412	1.5341	0.1071	1.6418	1.5341	0.1077
1.072	1.6449	1.5327	0.1122	1.6417	1.5332	0.1085	1.6427	1.5330	0.1097
1.085	1.6455	1.5313	0.1142	1.6423	1.5324	0.1099	1.6435	1.5325	0.1110
1.096	1.6463	1.5312	0.1151	1.6427	1.5317	0.1110	1.6438	1.5316	0.1122
1.113	1.6465	1.5315	0.1150	1.6435	1.5305	0.1130	1.6444	1.5308	0.1136
1.120	1.6465	1.5313	0.1152	1.6436	1.5302	0.1134	1.6445	1.5306	0.1139

The expected error in $n^{\parallel}$ and $n^{\perp}$ is ± 0.0007.

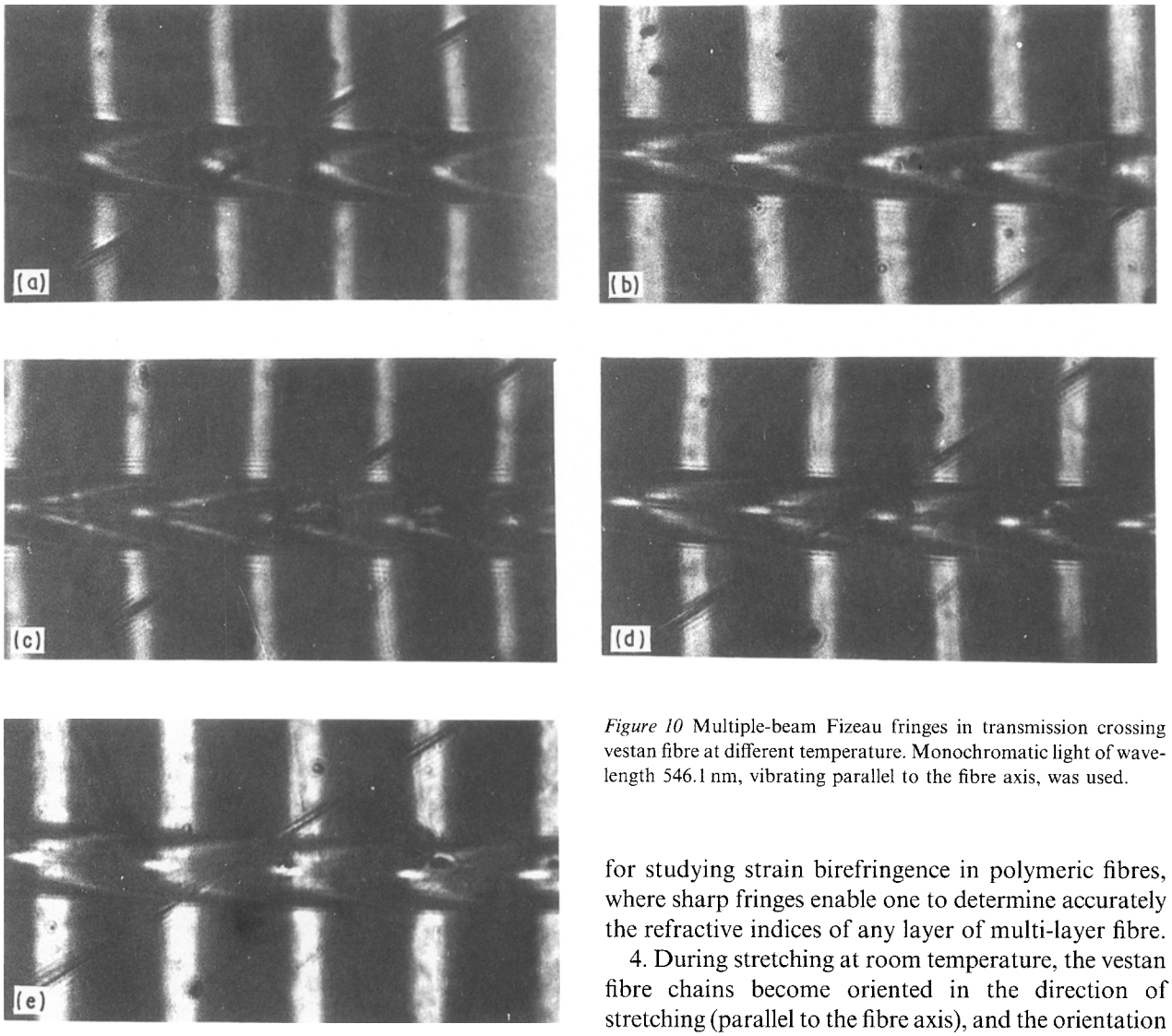

Figure 10 Multiple-beam Fizeau fringes in transmission crossing vestan fibre at different temperature. Monochromatic light of wavelength 546.1 nm, vibrating parallel to the fibre axis, was used.

2. The use of multiple-beam Fizeau fringes verifies the Cauchy's dispersion formula and determines the constants A and B of this formula for each layer of the fibre.

3. Reliable results are obtained using the micro-strain device attached to the optical system. This produces multiple-beam Fizeau fringes in transmission for studying strain birefringence in polymeric fibres, where sharp fringes enable one to determine accurately the refractive indices of any layer of multi-layer fibre.

4. During stretching at room temperature, the vestan fibre chains become oriented in the direction of stretching (parallel to the fibre axis), and the orientation of the skin molecules differs from the chains of the core layer (see Figure 8). The core refractive index, $n_c^{\parallel}$ reaches saturation, while that of the skin, $n_s^{\parallel}$, does not. This may be caused by (a) the molecules of the undrawn core being more oriented than those of the undrawn skin; or (b) the stretching effect on the orientation of the core molecules being higher than that on the skin molecules.

TABLE IV The polarizability per unit volume for vestan fibre layers at different draw ratios

Draw ratio	$P_c^{\parallel}$	$P_c^{\perp}$	ΔP_c	$P_s^{\parallel}$	$P_s^{\perp}$	ΔP_s	$P_a^{\parallel}$	$P_a^{\perp}$	ΔP_a
1.000	0.0861	0.0737	0.0124	0.0859	0.0740	0.0119	0.0860	0.0739	0.0121
1.024	0.0862	0.0739	0.0123	0.0860	0.0740	0.0120	0.0861	0.0740	0.0121
1.028	0.0863	0.0739	0.0124	0.0860	0.0740	0.0120	0.0861	0.0740	0.0121
1.048	0.0863	0.0741	0.0122	0.0861	0.0742	0.0119	0.0861	0.0741	0.0120
1.056	0.0864	0.0742	0.0122	0.0861	0.0742	0.0119	0.0862	0.0742	0.0120
1.072	0.0865	0.0744	0.0121	0.0862	0.0743	0.0119	0.0863	0.0742	0.0121
1.085	0.0866	0.0745	0.0121	0.0863	0.0744	0.0119	0.0864	0.0743	0.0121
1.096	0.0867	0.0746	0.0121	0.0863	0.0745	0.0118	0.0864	0.0744	0.0120
1.113	0.0867	0.0745	0.0122	0.0864	0.0746	0.0118	0.0865	0.0745	0.0120
1.120	0.0867	0.0745	0.0122	0.0864	0.0747	0.0117	0.0865	0.0746	0.0119

TABLE V The thermal coefficient of refractive index for vestan fibre layers

Temperature range (°C)	$\frac{dn_c^{\parallel}}{dT}$ (°C^{-1})	$\frac{dn_s^{\parallel}}{dT}$ (°C^{-1})	$\frac{dn_a^{\parallel}}{dT}$ (°C^{-1})	$\frac{dn_c^{\perp}}{dT}$ (°C^{-1})	$\frac{dn_s^{\perp}}{dT}$ (°C^{-1})	$\frac{dn_a^{\perp}}{dT}$ (°C^{-1})
18–28	1.50×10^{-4}	1.76×10^{-4}	3.07×10^{-4}	1.00×10^{-4}	2.00×10^{-4}	1.67×10^{-4}
28–42	9.33×10^{-4}	1.76×10^{-4}	3.07×10^{-4}	1.00×10^{-4}	2.00×10^{-4}	1.67×10^{-4}

Expected error in measurement of temperature is ± 0.5° C.

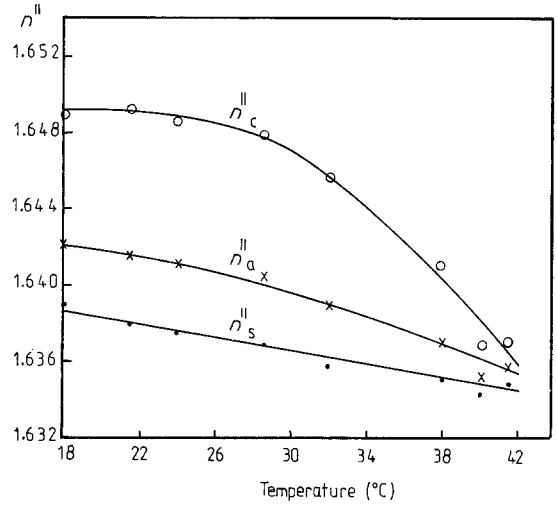

Figure 11 Variation of $n_s^{\parallel}$, $n_c^{\parallel}$ and $n_a^{\parallel}$ with temperature.

5. The determination of thermal coefficients of the refractive indices for vestan fibres with two layers (skin and core), (Table V) emphasizes the importance of the radiative properties of the skin and core media which define the fibre orientation, size distribution and relation with optical properties.

6. An empirical formula has been applied to relate the variation of birefringence with temperature, and the constants of this formula have been determined for each fibre layer.

7. As temperature increases, values of Δn_a, Δn_s and Δn_c decrease with variations of the thermal parameters. This verifies that molecular orientation decreases at high temperature.

8. The results obtained from the forward diffraction technique have been found to be more accurate and sensitive than those obtained by the other two methods used.

Since Δn_a, Δn_s, Δn_c, ΔP_a, ΔP_s and ΔP_c are a consequence of the material being drawn or thermally treated, so optical anisotropy is a consequence of thermo-mechanical anisotropy. We conclude that multiple-beam Fizeau fringes offer a valuable technique for gaining information on the thermal, mechanical and optical properties of the fibres.

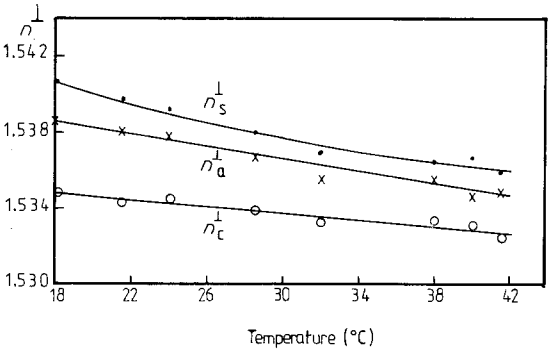

Figure 12 Variation of $n_s^{\perp}$, $n_c^{\perp}$ and $n_a^{\perp}$ with temperature.

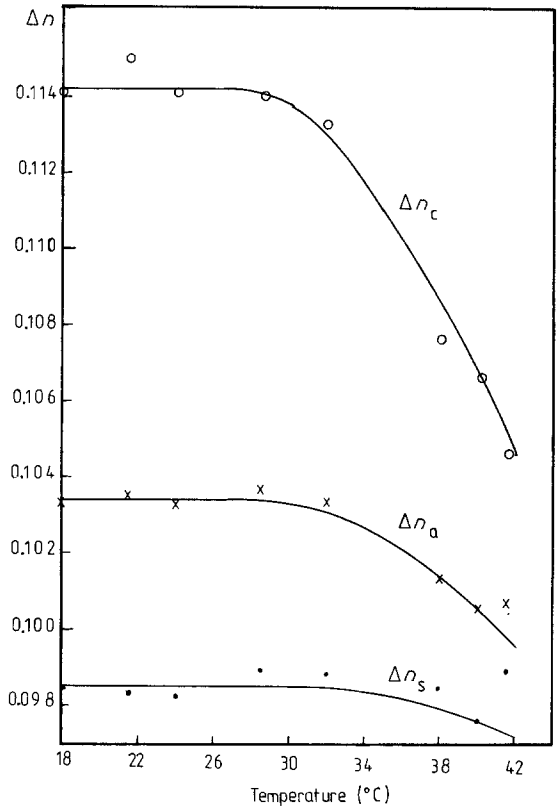

Figure 13 Fitting experimental points of the birefringence Δn_s, Δn_c and Δn_a with theoretical values (full curve) calculated using Equation 7.

References

1. J. R. SAMUELS, "Structured Polymer Properties" (Wiley, New York, 1974) p. 50.
2. R. H. PETER, "Textile Chemistry", Vol. 1 (Elsevier, London, 1963) p. 396.
3. N. BARAKAT and H. A. EL-HENNAWI, *Tex. Res. J.* **1** **41** (1971) 391.
4. M. PLUTA, *J. Microsc.* **96** (1972) 309.
5. M. M. EL-NICKLAWY and I. M. FOUDA, *J. Tex. Inst.* **71** (1980) 257.
6. I. M. FOUDA, K. A. EL-FARAHATY and K. A. EL-SAYED, *J. Mater. Sci.* **23** (1988) 3528.
7. I. M. FOUDA, M. M. EL-NICKLAWY, K. A. EL-FARAHATY and T. EL-DESSOUKI, *J. Text. Inst.* **5** (1987) 378.
8. I. M. FOUDA, M. M. EL-TONSY and A. H. ORABY, *J. Mater. Sci. Lett.* **8** (1989) 112.
9. I. M. FOUDA and M. M. EL-NICKLAWY, *Acta Phys. Polonica* **A59** (1981) 95.
10. A. A. HAMZA and M. A. KABEEL, *J. Phys. D: Appl. Phys.* **19** (1986) 1175.
11. I. M. FOUDA and M. M. EL-NICKLAWY, *J. Mater. Sci. Lett.* **7** (1988) 1136.
12. S. M. CURRY and A. L. SCHAWLOW, *Amer. J. Phys.* **42** (1974) 12.
13. I. M. FOUDA, T. EL-DESSOUKI and K. A. EL-FARAHATY, *Ind. J. Tex. Res.* **13** (1988) 11.
14. A. A. HAMZA, I. M. FOUDA, K. A. EL-FARAHATY and S. A. HELALY, *Polym. Test.* **7** (1987) 329.
15. S. C. LEE, *J. Quant. Spectrosc. Radiant Transfer* **36** (1986) 253.
16. R. H. PETER, *ibid.* **2** (1963) 393.

Received 16 February
and accepted 7 June 1989